

Newns-Anderson model of chemicurrents in H/Cu and H/Ag

M. S. Mizielinski^{a,*}, D. M. Bird^a,

^a*Department of Physics, University of Bath, Bath, BA2 7AY, UK*

M. Persson^b and S. Holloway^b

^b*Surface Science Research Centre, University of Liverpool, Liverpool, L69 3BX,
UK*

Abstract

The excitation of the electronic system induced by the adsorption of a hydrogen atom on the (111) surfaces of copper and silver is investigated using the time-dependent, mean-field Newns-Anderson model. Parameters for the model are obtained by fitting to density functional theory calculations, allowing the charge and energy transfer between adsorbate and surface to be calculated, together with the spectrum of electronic excitations. These results are used to make direct comparisons with experimental measurements of chemicurrents, yielding good agreement for both the magnitude of the current and the ratio of the currents for H and D adsorption.

Key words: Excitation spectra calculations, Chemisorption, Energy dissipation, Electron-hole pairs

PACS: 34.60.Dy, 68.43.-h, 73.20.Hb, 79.20.-m

1 Introduction

1 Until recently the direct observation of non-adiabatic dissipation of energy
2 into electronic excitations during adsorption events has been limited to highly
3 energetic processes, such as the oxidation of alkali and alkali-earth metals
4 [1]. Such reactions can result in chemiluminescence or the ejection of exo-
5 electrons. Investigation of low-energy electronic excitations has been restricted
6 by the difficulties involved in making experimental measurements. However,
7 two recent series of experiments have provided the first direct observations of
8 the excitation of relatively low-energy electrons and holes. White, Wodtke and
9 co-workers [2–4] observed exo-electron excitation when a low-workfunction,
10 caesium-doped gold surface was exposed to a beam of vibrationally excited
11 NO molecules. They suggested that during the vibration of the NO molecules
12 the ground electronic state oscillates between the neutral and negative ion and
13 rapid transfer of an electron between the surface and the molecule during this
14 oscillation leads to the excitation of the electronic system [3].

15 Here we are interested in the chemicurrent experiments performed by Nien-
16 haus and coworkers [5–9]. These experiments involve the fabrication of Schot-
17 tky diodes, consisting of a thin, ~ 100 Å, metal film deposited onto a doped
18 silicon wafer with electrical contacts made to the film and the back of the
19 wafer. On exposure to beams of atomic hydrogen, hot electrons or holes with
20 sufficient energy to traverse the metal film and cross the Schottky barrier
21 at the metal-semiconductor interface were measured as a chemically-induced-
22 reverse-current or ‘chemicurrent’. These devices have been used to investigate

* Corresponding author

Email address: M.S.Mizielinski@bath.ac.uk (M. S. Mizielinski).

23 differences in the adsorption of hydrogen isotopes [5,9] as well as a range of
24 other adsorbates [6,8]. Similar devices have also been used to study other sur-
25 face phenomena [10] including adsorption and desorption in H/Au [11] and
26 chemiluminescence in O/Mg [12].

27 Theoretical modelling of the electronic excitations generated during the ad-
28 sorption of hydrogen atoms on metal surfaces has been performed recently
29 using three techniques: electronic friction based methods [13–17], the time-
30 dependent, mean-field Newns-Anderson model [18–24] and time-dependent
31 density functional theory (TDDFT) [25–27].

32 Electronic friction methods use a nearly-adiabatic approximation in which the
33 time-dependent perturbation of the electronic system is assumed to be weak
34 and slow. This leads to a description of energy transfer equivalent to that
35 induced by a simple frictional force. The electronic friction coefficient can be
36 calculated through ab-initio methods [13], and has been widely used in the
37 study of surface dynamics, including the damping of vibrations in adsorbed
38 molecules [14] and desorption dynamics [15]. The energy distribution of excited
39 electron-hole pairs can be obtained by coupling this friction description to the
40 forced oscillator model [16,17].

41 However, electronic friction calculations exhibit problematic features when
42 considering strongly non-adiabatic behaviour. Trail and coworkers [16,17]
43 found that ab-initio calculations of the friction coefficient for an H-atom above
44 a copper (111) surface yield a singularity at an altitude of 2.4 Å above the
45 atop site. This unphysical feature was linked to the change in the ground
46 state from being spin-polarised (H-atom far from the surface) to unpolarised
47 (H-atom close to the surface). To avoid this problem a somewhat arbitrary

48 choice was made to constrain the spin of the DFT calculations to be constant,
49 giving a non-singular variation for the friction coefficient. Calculations using
50 these constrained results yielded probabilities for electrons being excited over
51 a Schottky barrier which were in line with the experimental results of Nien-
52 haus and coworkers. The use of a spin-constrained calculation is not, however,
53 a satisfactory solution to the problem, and other methods have been sought
54 which can describe systems which experience a spin-transition.

55 The time-dependent, mean-field Newns-Anderson model [18, 19], used in our
56 previous work [20–23], provides a straightforward way to study the spin-
57 transition in a fully non-adiabatic fashion. This model describes the interaction
58 of a single adsorbate orbital, containing a pair of coupled energy levels, with a
59 broad band of metal states. Time-dependence is included through the move-
60 ment of the adsorbate energy levels relative to the Fermi level and the variation
61 of the adsorbate-metal interaction. Within the mean-field and wide-band ap-
62 proximations expressions describing the time-evolution of the adsorbate energy
63 level occupations, the non-adiabatic transfer of energy to the surface [21, 23],
64 and the spectrum of electronic excitations have been derived [22, 23].

65 TDDFT calculations take the set of Kohn-Sham wavefunctions for a given
66 system, generated from a conventional static DFT calculation, and evolve
67 them through the time-dependent Schrödinger equation, using Ehrenfest dy-
68 namics for the nuclear motion. This technique has been used by Lindenblatt
69 and Pehlke [25–27] to investigate the interaction of hydrogen atoms with an
70 aluminium surface, yielding results for the non-adiabatic energy transfer and
71 the spectrum of electronic excitations. However, computational constraints re-
72 strict the application of this technique to consideration of light elements only,
73 and the restricted basis set leads to somewhat noisy results. A recent com-

74 parison of TDDFT and Newns-Anderson results for the H/Al system [24] has
75 shown good agreement in these two descriptions of non-adiabatic behaviour.

76 In our previous publications we have introduced and demonstrated the prop-
77 erties of the time-dependent, mean-field Newns-Anderson model [21, 22] us-
78 ing simple parameter variations to explore the non-adiabatic evolution of the
79 adsorbate-metal system. Here, we use this model to analyse systems of di-
80 rect relevance to the chemicurrent experiments described above: hydrogen
81 and deuterium atoms approaching the copper and silver surfaces. This work is
82 presented in two steps. In section 2 the method used to generate appropriate
83 parameters for the H/Cu and H/Ag systems is described. These parameters
84 are then used in section 3 to make comparisons between theoretical and ex-
85 perimental results for both the size of the chemicurrent and isotopic ratios on
86 each metal surface. Conclusions are drawn from these results in section 4.

87 **2 Parameterisation of the Newns-Anderson model**

88 Within the wide-band and mean-field approximations the Newns-Anderson
89 model can be parameterised through the position of the bare adsorbate level
90 ϵ_a , the width of the adsorbate resonance Γ and the intra-adsorbate Coulomb
91 repulsion energy U [18, 21–23]. Values of these parameters, as a function of
92 H-atom altitude, are found by fitting the adiabatic solution of the mean-
93 field Newns-Anderson model to ground-state DFT calculations. The time-
94 dependence is then obtained by choosing a trajectory which links altitude to
95 time in a realistic way.

96 A series of DFT calculations of hydrogen atoms above the copper and silver

97 (111) surfaces have been performed using the CASTEP [29] code. The surfaces
 98 were modelled with a slab geometry consisting of five layers of atoms and an
 99 equivalent vacuum gap above, with lattice parameters fixed at the experimen-
 100 tal bulk values of 3.614 Å and 4.085 Å for copper and silver respectively [28].
 101 The hydrogen atom was placed at a set of altitudes above an atop site of the
 102 surface. Both systems were represented using a 2×2 in-plane supercell, and
 103 ultra-soft pseudopotentials were used for both the metal and the hydrogen
 104 atoms. The Perdew-Burke-Ernzerhof (PBE) exchange-correlation functional
 105 was used, and a Fermi surface smearing of 0.25 eV was applied. Sampling of
 106 the surface Brillouin zone was performed using 54 k-points, and plane-wave
 107 cutoffs of 290 eV and 300 eV were used for the copper and silver surfaces
 108 respectively.

109 A total of 88 calculations were performed for the two systems with H-atom
 110 altitudes varied between 1 and 3.5 Å. The potential energy curves and the
 111 spin-polarisation are plotted in Fig. 1. Panel (b) shows the square-root like,
 112 second-order transition in the spin-polarisation of the hydrogen-metal systems,
 113 a characteristic of mean-field theories. At each altitude the projected density
 114 of states (PDOS) onto the hydrogen 1s orbital is calculated for fitting to the
 115 Newns-Anderson model. In the adiabatic limit of the wide-band, mean-field
 116 Newns-Anderson model the two adsorbate resonances, one for each spin σ ,
 117 are Lorentzian in shape with width Γ , centred on the effective energy levels
 118 $\bar{\epsilon}_{a\sigma}^{(ad)}$ [21]. From the PDOS, fitted values for Γ and $\bar{\epsilon}_{a\sigma}^{(ad)}$ have been extracted
 119 and are plotted in Figs 2(a)-(d). While these results could be used directly
 120 to obtain a variation for the bare energy level ϵ_a and the value of U , it is
 121 important to consider whether this would provide the best description of the
 122 excitation process in the H/Cu and H/Ag systems. In previous work [22,23] we

123 have shown that the transfer of charge between the adsorbate and surface can
 124 significantly alter the excitation spectrum. An excess of high-energy electrons
 125 is produced if there is a net electron transfer to the surface, while an excess
 126 of high-energy holes is generated if adsorption is accompanied by electron
 127 transfer to the adsorbate. It is therefore important that the occupations of the
 128 adsorbate level are correctly represented in order to obtain reliable results.

129 We have therefore devised a procedure which gives parameterisations of Γ
 130 and ϵ_a , and the value of U , which are consistent with a desired variation
 131 of the adsorbate level occupation. The target occupations are calculated by
 132 integrating the DFT generated H-atom PDOS up to the Fermi level, and are
 133 shown in Figs 2(e) and (f). Error functions are then used to fit the variation of
 134 the resonance width and bare energy level with altitude, with the constraint
 135 that the adsorbate occupations are consistent with those obtained from the
 136 DFT PDOS. The procedure for obtaining these parameters is described in
 137 detail in Ref. [24], and yields the following results for the H/Cu and H/Ag
 138 systems;

$$\text{H/Cu : } \frac{\epsilon_a}{\text{eV}} = -2.872 - 0.263 \operatorname{erfc} \left(3.717 \left(\frac{s}{\text{\AA}} - 1.729 \right) \right), \quad (1a)$$

$$\frac{\Gamma}{\text{eV}} = -8.020 \times 10^{-5} + 2.805 \operatorname{erfc} \left(1.796 \left(\frac{s}{\text{\AA}} - 2.352 \right) \right), \quad (1b)$$

$$\frac{U}{\text{eV}} = 4.827, \quad (1c)$$

139

$$\text{H/Ag : } \frac{\epsilon_a}{\text{eV}} = -2.774 - 0.430 \operatorname{erfc} \left(4.076 \left(\frac{s}{\text{\AA}} - 1.901 \right) \right), \quad (2a)$$

$$\frac{\Gamma}{\text{eV}} = -1.748 \times 10^{-3} + 2.944 \operatorname{erfc} \left(1.514 \left(\frac{s}{\text{\AA}} - 2.396 \right) \right), \quad (2b)$$

$$\frac{U}{\text{eV}} = 4.574, \quad (2c)$$

141 where s is the altitude of the H-atom above the atop site. These variations
 142 are plotted, along with the fits to the DFT PDOS in Figs 2(a)-(d), with the
 143 resulting adsorbate level occupations in panels (e) and (f).

144 To complete the parameterisation of the Newns-Anderson model we require
 145 the variation of Γ and ϵ_a with time. We have chosen to use a constant total
 146 energy trajectory with an initial kinetic energy at 4 Å of 25 meV, where the
 147 H-atom is accelerated in the potential energy curves shown in Fig 1. As we
 148 are particularly interested in the effects of the spin-transition, calculations are
 149 terminated when the adsorbate reaches the back of the surface potential well,
 150 i.e when the adsorbate reaches 1.1 Å or 1.25 Å for the copper and silver surfaces
 151 respectively. Isotope effects (explored experimentally by Krix, Nienhaus and
 152 co-workers [9]) can be investigated by changing the adsorbate mass in the
 153 trajectory calculations.

154 **3 Results**

155 In this section we use the parameters derived above and the computational
 156 model described previously [21–23] to investigate the non-adiabatic behaviour
 157 of the H/Cu and H/Ag systems. In addition to $\Gamma(t)$, $\epsilon_a(t)$ and U , the computa-
 158 tion of the adsorbate occupations, energy transfer rates and excitation spectra
 159 requires a set of energy grids for the evaluation of integrals. Here, a 128,001
 160 point energy grid covering the range -90 to 10 eV relative to the Fermi level
 161 has been used with numerical methods equivalent to those discussed previ-
 162 ously [22, 23]. A system temperature of 175 K is used in all calculations.

163 Fig. 3 shows the time-evolving charge and energy transfer behaviour for hy-
 164 drogen and deuterium atoms approaching the copper and silver (111) surfaces.
 165 As the adsorbates approach the metal surfaces the adiabatic occupations for
 166 the majority and minority spins converge on one another resulting in a sharp
 167 spin transition at 2.3-2.4 Å. The time-dependent occupations overshoot this
 168 spin-transition, with smaller differences $n_{a\sigma} - n_{a\sigma}^{(ad)}$ for the slower deuterium
 169 atoms in comparison with those for hydrogen. Associated with this overshoot
 170 of the adiabatic spin-transition is a non-adiabatic transfer of energy to the
 171 metal surface, the rate of which is shown in panels (b) and (d) of Fig. 3. Each
 172 system shows a sharp peak in this energy transfer rate at the spin transition
 173 with a small secondary peak (most prominent for the silver surface) just below
 174 2 Å. This secondary peak is driven by the variation of the bare adsorbate level
 175 ϵ_a , (see Figs. 2(c) and (d)), while the large increase in Γ is responsible for most
 176 of the non-adiabatic behaviour close to the spin-transition.

177 By integrating over each trajectory the energy dissipated into electron-hole
 178 pairs during the approach to the surface can be obtained. We find that H (D)
 179 atoms approaching the copper surface deposit 115 meV (88 meV), and those
 180 approaching the silver surface deposit 105 meV (80 meV). It is important to
 181 note that these energy transfers are expectation values and as such are an
 182 average over many trajectories. It is therefore possible for an electron hole-
 183 pair to have more energy than this average energy transfer, but with a limited
 184 probability.

185 The spectrum of electronic excitations generated by the approach of the ad-
 186 sorbing hydrogen atom is plotted in Fig. 4 for each of the four systems under
 187 consideration. The effects due to the majority and minority spins have been
 188 summed in these spectra. Each spectrum consists of a pair of sharp peaks close

189 to the Fermi level, with electrons being excited just above ϵ_F and holes just
190 below. Away from the Fermi level, i.e. $|\epsilon - \epsilon_F| \geq 0.2$ eV, the excitation spec-
191 tra falls off roughly exponentially with energy for both electrons and holes.
192 The shape of the different sections of the excitation spectra, their dependence
193 on the parameters of the system and the impact of temperature have been
194 explored previously [22, 23].

195 The isotope effect for the two systems, i.e. the difference between the excitation
196 spectra for hydrogen and deuterium atoms, appears to be small on the linear
197 scales used in panels (a) and (b) of Fig. 4. However, the semi-logarithmic scales
198 used to display the same data in panels (c) and (d) show that the probability
199 of high-energy excitations falls roughly exponentially, with different rates for
200 the two isotopes. It has become conventional [9, 24–26] to describe these distri-
201 butions using Boltzmann factors with an effective temperature $T^{(\text{eff})}$. Values
202 for $T^{(\text{eff})}$ have been extracted from each of the spectra shown in Fig. 4 and
203 are presented in Table 1. These data show that the differences between the
204 two metal surfaces are small, while the isotope effect is significant. TDDFT
205 and Newns-Anderson model calculations for the H/Al(111) system [24] yield
206 effective temperatures in the range 1400-1700 K, which is similar to those
207 obtained here.

208 The results presented in Fig. 4 can be used to estimate the chemicurrents mea-
209 sured in the thin-film Schottky diode experiments of Nienhaus and cowork-
210 ers [5]. The probability of exciting electrons and holes, $P_e^{(\text{chemi})}$ and $P_h^{(\text{chemi})}$,
211 with sufficient energy to be detected in such devices can be estimated by

Table 1

Effective temperatures for electrons and holes for the spectra plotted in Fig 4. Uncertainties in these values arising from the least-squares fitting procedure are approximately ± 10 K.

System	H/Cu	D/Cu	H/Ag	D/Ag
$T^{(\text{eff})}$ (electrons)	1400 K	1160 K	1370 K	1110 K
$T^{(\text{eff})}$ (holes)	1470 K	1160 K	1410 K	1150 K

$$P_e^{(\text{chemi})}(\epsilon > \epsilon_S) = \int_{\epsilon_S}^{\infty} d\epsilon n^{(ex)}(\epsilon) a(\epsilon, \epsilon_S), \quad (3)$$

$$P_h^{(\text{chemi})}(\epsilon > \epsilon_S) = \int_{\epsilon_S}^{\infty} d\epsilon |n^{(ex)}(-\epsilon)| a(\epsilon, \epsilon_S), \quad (4)$$

212 where ϵ_S is the Schottky barrier height, $n^{(ex)}(\epsilon)$ is the total excitation spec-
 213 trum and $a(\epsilon, \epsilon_S)$ is a geometrical factor, which contains two components.
 214 The first describes the attenuation of hot electrons or holes as they propa-
 215 gate through the metal film, while the second describes the probability, given
 216 isotropic emission of the electrons from the adsorption site (within the metal),
 217 that the electron or hole has sufficient normal energy to cross the Schottky
 218 barrier at the metal-silicon interface. The factor a can be expressed as

$$a(\epsilon, \epsilon_S) = \int_0^{\theta_c} d\theta \sin(\theta) \exp \left[-\frac{D}{\lambda \cos(\theta)} \right], \quad (5)$$

219 where θ is the angle to the surface normal and $\theta_c = \cos^{-1} \sqrt{\epsilon_S/\epsilon}$ is the angle
 220 above which the electron or hole will not have enough normal energy to cross
 221 the Schottky barrier. λ is the mean free path of electrons (assumed to be
 222 independent of energy) within the metal film, which has a thickness D . In
 223 using these expressions a number of additional assumptions are being made:

224 there is no preference for the direction of propagation of the excitations within
225 the metal, the metal has a uniform thickness and the Schottky barrier height is
226 uniform throughout the device. The probability that an electron with sufficient
227 normal energy is able to cross the Schottky barrier is also assumed to be unity.

228 The probability of detecting an electron or a hole in a thin-film Schottky de-
229 vice is plotted in Fig. 5. Mean-free paths for electrons and holes were taken
230 to be 100 Å [5] for copper and 240 Å [9] for silver. A film thickness of 75
231 Å was also assumed for both metal films [5]. The magnitude of the chemi-
232 currents measured in the experiments of Nienhaus and coworkers compares
233 well with these results. Experiments using Cu/n-Si(111) devices, with a 0.6
234 eV Schottky barrier, measured 1.5×10^{-4} electrons per incident H-atom [5].
235 Our model suggests approximately 0.9×10^{-4} electrons per atom for the single
236 approach to the surface simulated. Krix, Nünthel and Nienhaus have recently
237 performed a detailed study of Ag/p-Si(111) devices which have a well char-
238 acterised Schottky barrier height of 0.46 eV [9]. On exposure to beams of
239 hydrogen and deuterium atoms chemicurrents in the range $1-10 \times 10^{-4}$ and $1-$
240 5×10^{-4} holes per atom were measured respectively. These data also compare
241 well to our model – we estimate chemicurrent yields of 4.8×10^{-4} (1.5×10^{-4})
242 holes per incident hydrogen (deuterium) atom.

243 There is, however, some uncertainty in experimental measurements of the ab-
244 solute chemicurrent yield due to difficulties in quantifying the flux of atoms
245 reaching the device surface. One quantity which is insensitive to this uncer-
246 tainty is the ratio of the chemicurrents generated by beams of hydrogen and
247 deuterium atoms. Krix and co-workers reported that the chemicurrents for
248 hydrogen are 3.7 ± 0.7 times larger than for deuterium for their Ag/p-Si (111)
249 devices [9]. The first experimental report of chemicurrents by Nienhaus and

250 coworkers [5] also estimated the ratio of chemicurrents for Ag/n-Si and Cu/n-
251 Si devices, giving an electron chemicurrent ratio of approximately six for bar-
252 rier heights in the range 0.5-0.6 eV. To compare our calculations with these
253 results the ratio of chemicurrents generated by H and D-atoms has been plot-
254 ted in Fig. 6 for both copper and silver films. For an Ag/p-Si device with a
255 barrier height of 0.46 eV our model yields a ratio of H:D hole chemicurrents
256 of 3.2:1, while an Ag/n-Si device with barrier heights in the range 0.5-0.6 eV
257 gives ratios between 4.1:1 and 5.4:1. Both results are in good agreement with
258 those reported by Nienhaus, Krix and co-workers.

259 4 Conclusions

260 The Newns-Anderson model provides a simple but effective method for analysing
261 non-adiabatic processes in adsorption at surfaces. It allows for the calculation
262 of strongly non-adiabatic effects, such as those occurring at a spin transition.
263 Its simplicity means that, for any set of parameter variations, the calculation
264 of charge and energy transfer rates and the spectrum of electronic excitations
265 is quick and straightforward.

266 The key result of this paper is that a single passage of the hydrogen atom
267 adsorbate through the spin transition yields a significant energy transfer into
268 electronic excitations, and sufficient numbers of high energy excitations to
269 account for the chemicurrent measured in thin-film Schottky devices. This
270 leaves open the question of the effect on the chemicurrent yield of the remain-
271 der of trajectory, as the atom undergoes damped vibrations in the surface
272 potential well. It is possible to run the Newns-Anderson model for such a
273 trajectory, with the damping rate being derived either from the energy loss

274 in the Newns-Anderson model itself, or using an ab-initio friction coefficient
275 as in [17]. However, a problem arises because, at least for the first few os-
276 cillations, the hydrogen atom passes through the spin transition both when
277 moving towards and moving away from the surface. The latter case is where
278 the difficulty emerges.

279 If we consider the first rebound of the atom within the potential well, it can
280 be seen from Fig. 3 that the atom has de-polarised by the time it reaches
281 the back wall and we find that the spin polarisation is zero (to numerical
282 accuracy) by the time the atom passes back through the altitude where the
283 spin transition occurs. At this point, the atom can re-polarise, but within our
284 numerical model there is nothing to determine in which direction the majority
285 spin will be. The re-polarisation occurs in an unpredictable and irreproducible
286 way, because it is driven by numerical instability. We do not believe that this
287 can be regarded as representing a physical reality. An alternative treatment is
288 to keep the atom non-polarised for the remainder of the trajectory after the
289 first approach to the surface, and to analyse non-adiabaticity by comparing the
290 time-dependent solution with a non-polarised adiabatic state (a metastable,
291 non-polarised adiabatic solution exists even when the ground state is spin
292 polarised). We have performed such calculations, and the results show that
293 the full trajectory gives an excitation spectrum whose magnitude is a factor
294 of about two or three times that shown in Fig. 4. However, the justification
295 for using this treatment is not clear; for example, if the atom could escape
296 from the surface the method cannot be right because the final state of the
297 atom should be spin polarised. The correct way to handle re-polarisation of
298 the atom as it leaves the surface remains an open question, and one that is
299 as relevant to ab-initio approaches like TDDFT as it is to model calculations

300 like the ones presented here.

301 **Acknowledgments**

302 Financial support from the Engineering and Physical Sciences Research Coun-
303 cil (EPSRC), Grant No. EP/E021646/1, is gratefully acknowledged.

304 **References**

- 305 [1] Greber T., *Surf. Sci. Rep.* **28**, 1 (1997).
- 306 [2] White J. D., Chen J., Matsiev D., Auerbach D. J. and Wodtke A. M., *Nature*
307 **433**, 503 (2005).
- 308 [3] White J. D., Chen J., Matsiev D., Auerbach D. J. and Wodtke A. M., *J. Chem.*
309 *Phys.* **124**, 064702 (2006).
- 310 [4] A. M. Wodtke, D. Matsiev and D. J. Auerbach, *Prog. Surf. Sci.* (submitted).
- 311 [5] Nienhaus H., Bergh H. S., Gergen B., Majumdar A., Weinberg W. H. and
312 McFarland E. W., *Phys. Rev. Lett.* **82**, 446 (1999).
- 313 [6] Gergen B., Nienhaus H., Weinberg W. H. and McFarland E. W., *Science* **294**,
314 2521 (2001).
- 315 [7] Nienhaus H., Gergen B., Weinberg W. H. and McFarland E. W., *Surf. Sci.* **514**,
316 172 (2002).
- 317 [8] Nienhaus H. *Surf. Sci. Rep.* **45**, 3 (2002).
- 318 [9] Krix D., Nünthel R. and Nienhaus H., *Phys. Rev. B* **75**, 073410 (2007).
- 319 [10] Hasselbrink E., *Curr. Opin. Solid St. M.* **10**, 192 (2006).

- 320 [11] Mildner B., Hasselbrink E. and Diesing D., *Chem. Phys. Lett.* **432**, 133 (2006).
- 321 [12] Nienhaus H. and Glass S., *Surf. Sci.* **600**, 4285 (2006).
- 322 [13] Trail J. R., Graham M. C. and Bird D. M., *Comp. Phys. Comm.* **137**, 163
323 (2001).
- 324 [14] Persson M., *Philos. Trans. R. Soc. London, Ser. A* **362** (1819), 1173 (2004).
- 325 [15] Luntz A. C. and Persson M., *J. Chem. Phys.* **123**, 074704 (2005).
- 326 [16] Trail J. R., Graham M. C., Bird D. M., Persson M. and Holloway S., *Phys. Rev.*
327 *Lett.* **88**, 166802 (2002).
- 328 [17] Trail J. R., Bird D. M., Persson M. and Holloway S., *J. Chem. Phys.* **119**, 4539
329 (2003).
- 330 [18] Anderson P. W., *Phys. Rev.* **124**, 41 (1961).
- 331 [19] Newns D. M., *Phys. Rev.* **178**, 1123 (1969).
- 332 [20] Bird D. M., Persson M., Trail J. R. and Holloway S., *Surf. Sci.* **556-568**, 761
333 (2004).
- 334 [21] Mizielinski M. S., Bird D. M., Persson M. and Holloway S., *J. Chem. Phys.*
335 **122**, 084710 (2005).
- 336 [22] Mizielinski M. S., Bird D. M., Persson M. and Holloway S., *J. Chem. Phys.*
337 **126**, 034705 (2007).
- 338 [23] Mizielinski M. S., Ph.D. Thesis, University of Bath (2007).
- 339 [24] Bird D. M., Mizielinski M. S., Lindenblatt M. and Pehlke E., *Surf. Sci.* **602**,
340 1212 (2008),
- 341 [25] Lindenblatt M., Pehlke E., Duvenbeck A., Rethfeld B. and Wucher A., *Nucl.*
342 *Instrum. Meth. B* **246**, 333 (2006).

- 343 [26] Lindenblatt M. and Pehlke E., *Surf. Sci.* **600**, 2068 (2006).
- 344 [27] Lindenblatt M. and Pehlke E., *Phys. Rev. Lett.* **97**, 216101 (2006).
- 345 [28] D. R. Lide and H. P. R. Frederikse, *CRC Handbook of Chemistry and Physics*
346 (CRC Press Inc., 1994).
- 347 [29] M. D. Segall, P. J. D. Lindan, M. J. Probert, C. J. Pickard, P. J. Hasnip, S. J.
348 Clark and M. C. Payne, *J. Phys.: Condens. Matter*, **14**, 2717 (2002).

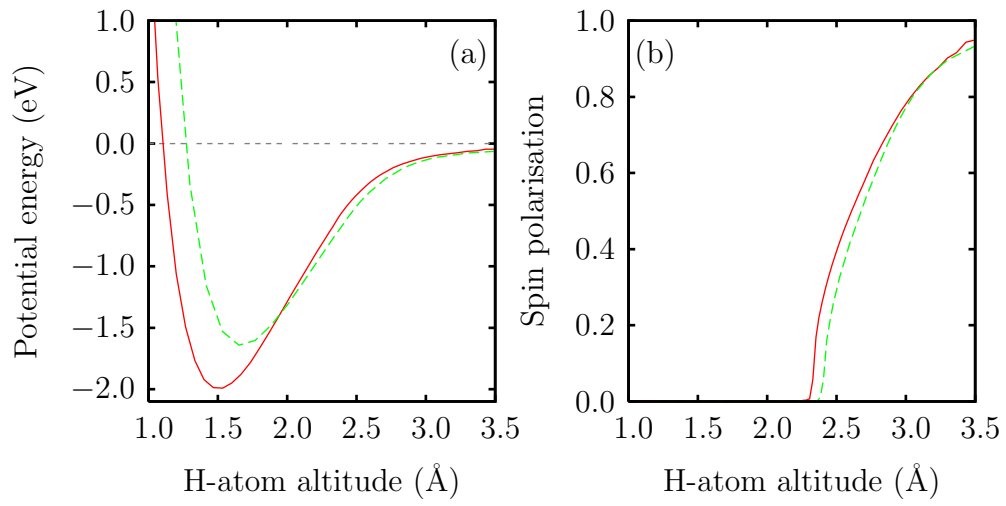


Fig. 1. (a) Surface potential well above the atop site and (b) spin polarisation of the H/Cu (solid-red lines) and H/Ag (dashed green lines) systems.

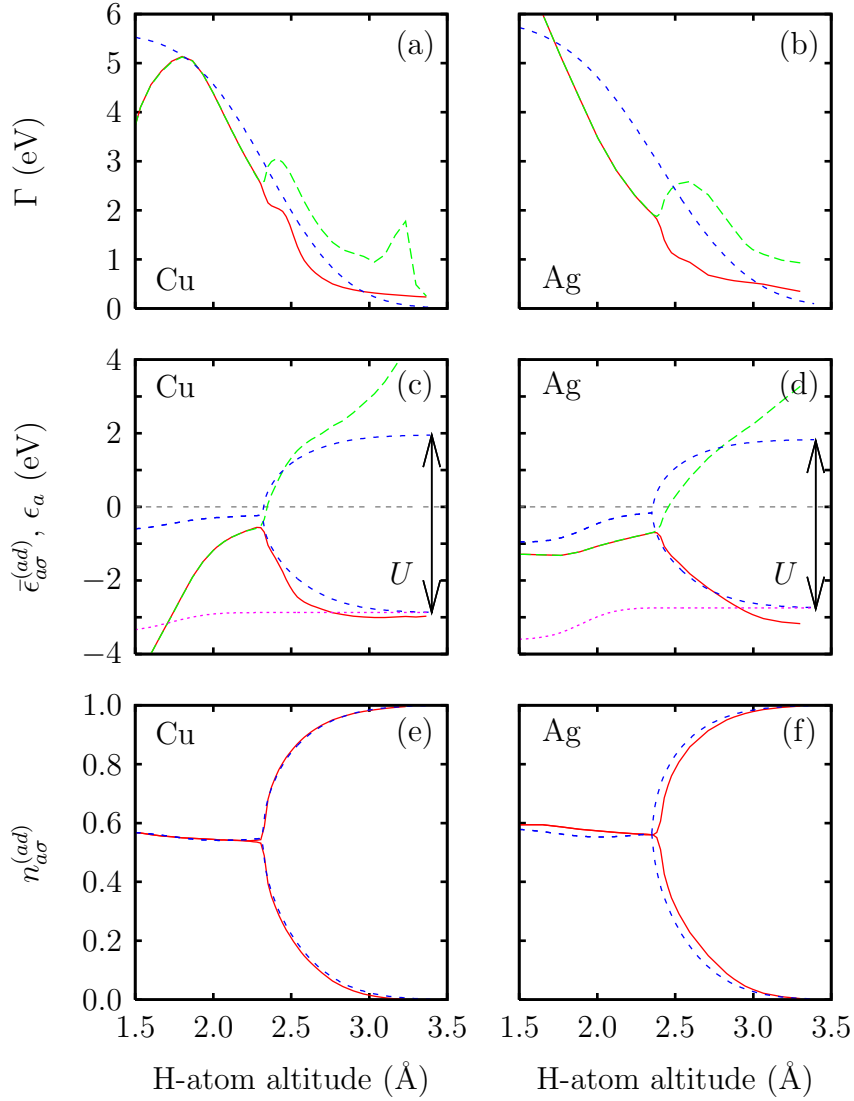


Fig. 2. Parameter variations for the H/Cu [(a), (c) and (e)] and H/Ag [(b), (d) and (f)] systems. In (a) and (b) solid red and long-dashed green lines denote the fitted resonance widths for majority and minority spin respectively, while the medium-dashed blue line denotes the error function fit used in later calculations. (c) and (d) show the energy levels with solid red (majority) and long-dashed green (minority) lines being fits to the DFT PDOS, and the medium-dashed blue and short-dashed magenta lines denoting the effective adsorbate energy level $\bar{\epsilon}_{a\sigma}^{(ad)}$ and the error function fit to ϵ_a respectively. Arrows in (c) and (d) indicate the value of U . The bottom two panels, (e) and (f), show the occupations of the adsorbate levels arising from the DFT calculations (solid red lines) and from the chosen parameter variations (medium-dashed blue lines).

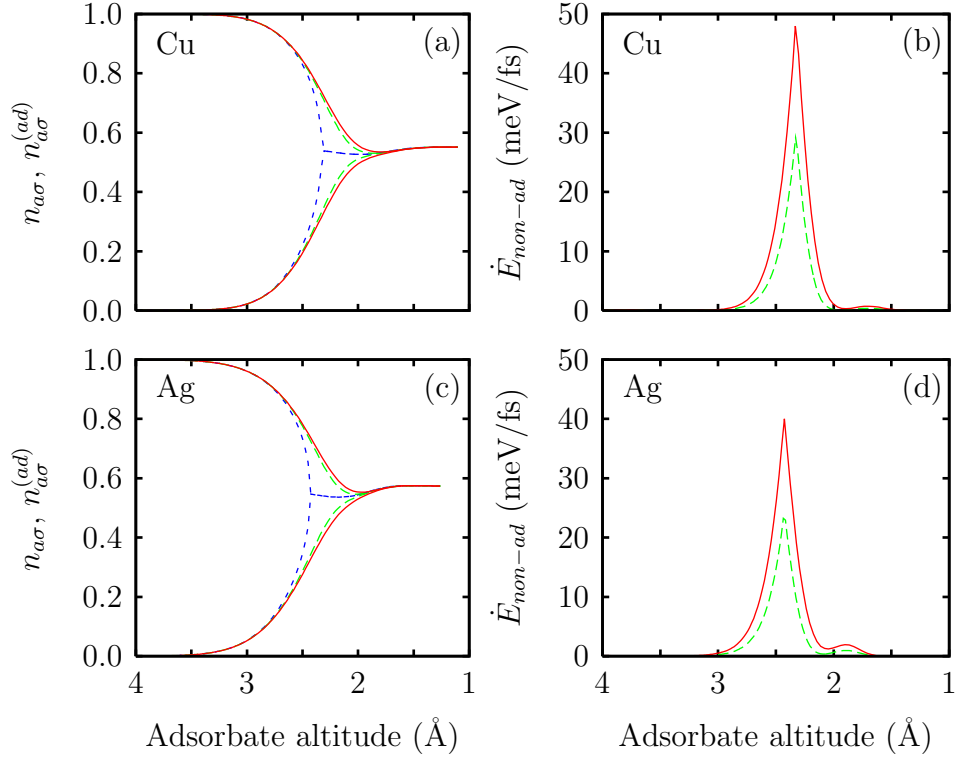


Fig. 3. Adsorbate level occupations, (a) and (c), and energy transfer rate, (b) and (d) as a function of altitude for hydrogen (solid red lines) and deuterium atoms (long-dashed green lines) approaching the copper, (a) and (b), and silver, (c) and (d), surfaces. Medium-dashed blue lines in panels (a) and (c) denote the adiabatic occupations for the two systems.

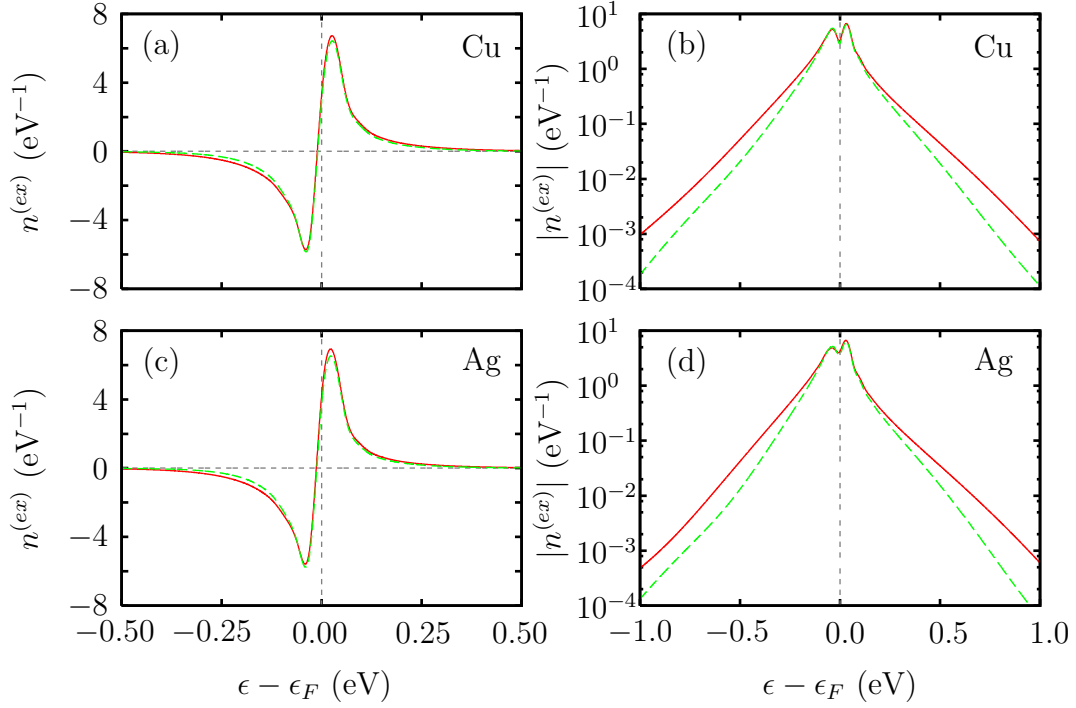


Fig. 4. Excitation spectra, $n^{(ex)}$, for hydrogen (solid red lines) and deuterium (dashed green lines) atoms upon reaching the turning point above the copper, panels (a) and (b), and silver, (c) and (d), surfaces. Panels (a) and (c) show spectra on linear scales, while a logarithmic scale for the excitation spectrum is used in panels (b) and (d) together with a larger energy range.

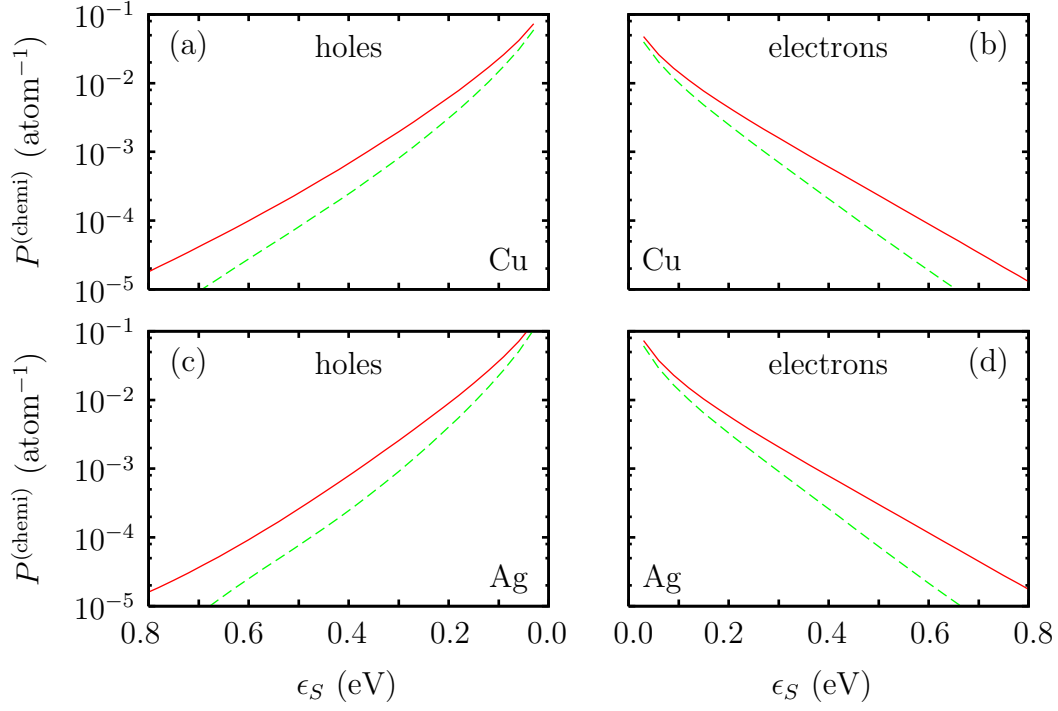


Fig. 5. Probability of measuring electrons and holes in a thin-film Schottky device as used by Nienhaus and co-workers. Panels (a) and (b) relate to Cu/Si devices, while (c) and (d) refer to Ag/Si devices. Electron probabilities are plotted in panels (b) and (d) with hole probabilities in (a) and (c). As previously, solid red lines refer to calculations for hydrogen atoms and dashed green lines to those for deuterium. A film thickness of 75 \AA was assumed with mean-free paths of 100 and 240 \AA for copper and silver surfaces respectively.

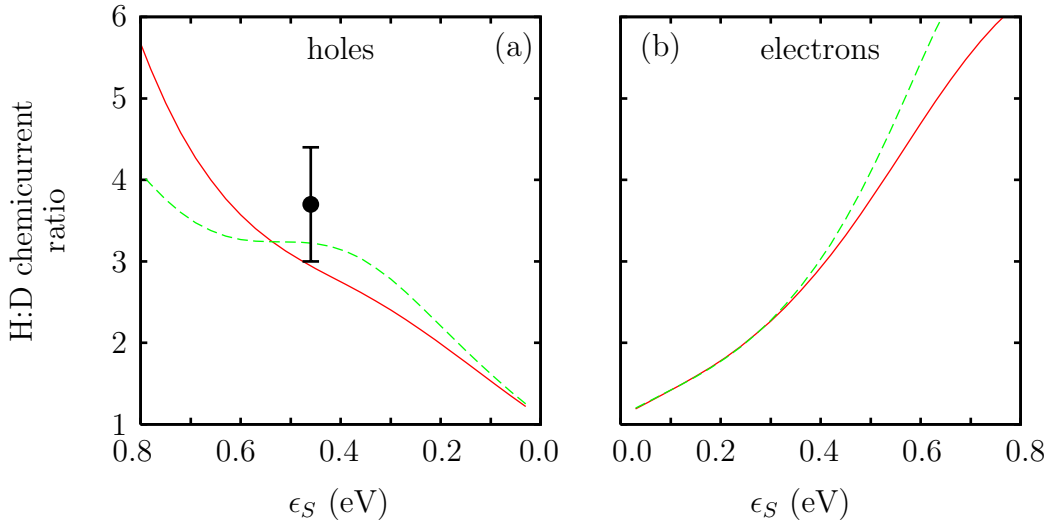


Fig. 6. H:D chemicurrent ratio, $P_H^{(\text{chemi})}/P_D^{(\text{chemi})}$, for the copper (solid red lines) and silver (long-dashed green lines) surfaces as a function of the Schottky barrier height. Panels (a) and (b) refer to hole and electron currents respectively. The point with error bars in (a) is the experimental result reported by Krix and co-workers [9].